M. A. SOKOLOVSKIY
Institute of Water Problems of the
Russian Academy of Sciences
3 Gubkina Str., 117735, Moscow, GSP-1, Russia
E-mail: sokol@aqua.laser.ru

J. VERRON
Laboratoire des Ecoulements
Géophysiques et Industriels
UMR 5519, CNRS, BP53 X
38041 Grenoble Cedex, France
E-mail: verron@hmg.inpg.fr

FOUR-VORTEX MOTION IN THE TWO LAYER APPROXIMATION: INTEGRABLE CASE

Received November 16, 2000 DOI: 10.1070/RD2000v004n04ABEH000157

The problem of four vortex lines with zero total circulation and zero impulse on a unlimited fluid plane, as it is known [4, 1, 16, 3], is reduced to a problem of three point vortices and is integrated in quadratures. In the given work these results are transferred on a case of four vortices in a two-layer rotating liquid. The analysis of phase trajectories of relative motion of vortices is made, and the singularities of absolute motion on an example of a head-on, off-center collision of two two-layer vortex pairs are studied. In particular, the new class of quasistationary solutions for the given type of motions is obtained. The problems of interaction of the distributed (or finite-core) two-layer vortices are discussed.

1. Introduction

It is known [13], that the velocity V of two vertical vortex lines with intensities identical in an absolute value, but with opposite signs (i. e. a vortex pair), in a homogeneous fluid on unlimited motionless (or rotating) horizontal liquid plane, is defined by a relation $V = \frac{s}{2\pi r}$, where s is the absolute value of intensity of each of the pair's vortex component, and r is the distance between vortices. The interaction of two vortex pairs (special case of four vortices with zero total intensity) is studied rather completely. The first results were obtained by Greenhill [13], where the case of the moment M equal to zero was considered. At $M \neq 0$ the picture of interaction of two pairs (and other combinations of four vortices with zero summarized intensity) is given in [1]. Let us assume:

1) The liquid consists of two layers with thicknesses h_1 and h_2 (non-perturbed condition) with constant densities ρ_1 and ρ_2 ($\rho_1 < \rho_2$);

2) For two vortex lines, located in different layers, with intensities s_1 and s_2 the condition of equality to zero of total circulation $h_1 s_1 + h_2 s_2 = 0$ is fulfilled.

Then, as shown in [8, 5], the velocity of such two-layer pair will be defined by a relation $V = \frac{\varkappa}{2\pi}\left[\frac{1}{r} - \gamma K_1(\gamma r)\right]$. Here $\varkappa = -h_1 s_1 = h_2 s_2 > 0$, $K_1(z)$ is the Bessel modified cylindrical function of the first order in the argument z; γ is a parameter, defining the stratification of the two-layer liquid (see the following section). In this case the distribution $V(r)$ represents non-monotonic function: $V \to 0$ both at $r \to \infty$, and at $r \to 0$, and reaches maximum value at $\gamma r \approx 1.114$ [17]. Owing to the hydrostatic equilibrium the vortices of *different* signs belonging to different layers, cause the

Mathematics Subject Classification 76C05

same sign deformations of interface between the layers. Thus, any two-layer pairs produces vertical *heat* redistribution. That's why Hogg and Stommel [8] have gave the name *hetons* to such two-layer vortices. In [8, 9] they have studied some cases of interaction of two and few hetons. The present work develops this subject. Below we shall name two-layer vortices, for which $r = 0$ as *hetons with vertical axes*. If $r \neq 0$, we shall speak about *hetons with tilted axes*.

2. Formulation of the problem

The motion of two two-layer point vortices on a plane rotating with constant angular velocity is described by a system of the ordinary differential equations [5, 8] written in the complex form

$$\frac{d\overline{z_m^n}}{dt} = \frac{1}{2\pi i}\Big\{\frac{\varkappa_m^{3-n}}{z_m^{3-n} - z_m^n}\Big[1 + \frac{h_{3-m}}{h_m}\gamma|z_m^{3-n} - z_m^n|K_1(\gamma|z_m^{3-n} - z_m^n|)\Big] + \\ + \sum_{j=1}^{2}\frac{\varkappa_{3-m}^j}{z_{3-m}^j - z_m^n}\Big[1 - \gamma|z_{3-m}^j - z_m^n|K_1(\gamma|z_{3-m}^j - z_m^n|)\Big]\Big\}, \tag{2.1}$$

Here $z_m^n = x_m^n + iy_m^n$ is a complex coordinate of n-th vortex from m-th layer (i. e. the superscript corresponds to the number of the two-layer vortex, and subscript corresponds to the number of the layer: 1 — upper layer, 2 — lower layer). This vortex has intensity $\varkappa_m^n = h_m s_m^n$. Remaining labels are the following: γ is a parameter, inversely proportional to the interior radius of Rossby deformation [15] $\lambda = [g(\rho_2 - \rho_1)h_1h_2/\rho_0 f^2(h_1 + h_2)]^{\frac{1}{2}}$, where g is a gravitational acceleration, ρ_0 is a average value of density, f is a the parameter of Coriolis assumed to be constant (it means, that the plane of Cartesian coordinates (x, y) rotates around perpendicular axis with constant angular velocity $f/2$); the overbar stands for the complex conjugate.

As it was said previously, the case $n = 1, 2$, $m = 1, 2$ is considered (two point vortices in each of two layers).

The system of four equations (2.1) has the following first integrals:

impulses

$$P = P_2 + iP_1 = \sum_{m=1}^{2}\sum_{n=1}^{2}\varkappa_m^n z_m^n \quad \text{and} \quad \overline{P} = P_2 - iP_1 = \sum_{m=1}^{2}\sum_{n=1}^{2}\varkappa_m^n \overline{z}_m^n, \tag{2.2}$$

where

$$P_1(P_2) = \sum_{m=1}^{2}\sum_{n=1}^{2}\varkappa_m^n y_m^n(x_m^n);$$

moment

$$M = \sum_{m=1}^{2}\sum_{n=1}^{2}\varkappa_m^n|z_m^n|^2, \tag{2.3}$$

Hamiltonian

$$H = -\frac{1}{2\pi}\sum_{m=1}^{2}\Big\{\varkappa_m^m\varkappa_m^{3-m}\Big[\ln|z_m^{3-m} - z_m^m| - \frac{h_{3-m}}{h_m}K_0(\gamma|z_m^{3-m} - z_m^m|)\Big] + \\ + \sum_{j=1}^{2}\varkappa_1^m\varkappa_2^j\Big[\ln|z_2^m - z_1^j| + K_0(\gamma|z_2^m - z_1^j|)\Big]\Big\}. \tag{2.4}$$

The Hamiltonian (2.4) represents the expression for a total interaction energy of elementary vortices. As Gryanik and Tevs [6] have shown, the invariance of interaction energy is stipulated by the values of the energy for separate layers that evolve in opposite phase. It is known [20, 3, 12, 14], that the system (2.1) generally is nonintegrable, and to make it integrable [20, 3], the integrals (2.2)–(2.3) must to be in involution, that has a place at

$$\varkappa = \sum_{m=1}^{2}\sum_{n=1}^{2}\varkappa_m^n = 0 \qquad \text{and} \qquad P = 0. \tag{2.5}$$

The first condition of (2.5) for the hetons is satisfied automatically. The second condition means, that each of four vortices in the initial instant moment (and identically, due to the invariant property of the quantity P, — identically) should be in the center of vorticity of remaining three vortices. Let us consider below the problems with the initial condition $P = 0$. Thus, all obtained solutions will have a regular character.

3. Analysis of relative motion

Following [1, 3], we shall consider the combination of integrals P and M:

$$L = \varkappa M - P^2 = \sum_{n=1}^{2}\Big(\varkappa_n^n\varkappa_n^{3-n}|z_n^{3-n} - z_n^n|^2 + \sum_{i=1}^{2}\varkappa_1^i\varkappa_2^n|z_2^n - z_1^i|^2\Big),$$

depending only on distances between the vortices $d_{ij}^{mn} = |z_j^n - z_i^m|$, and, it is obvious, that $L = 0$. After simple transformations we obtain equalities

$$\begin{aligned}
\varkappa_2^1\varkappa_2^2(d_{22}^{21})^2 &= \varkappa_1^1\varkappa_1^2(d_{11}^{21})^2 - (\varkappa_1^1 + \varkappa_1^2)M,\\
\varkappa_1^1\varkappa_2^2(d_{21}^{21})^2 &= \varkappa_1^2\varkappa_2^1(d_{21}^{12})^2 - (\varkappa_1^2 + \varkappa_2^1)M,\\
\varkappa_1^2\varkappa_2^2(d_{21}^{22})^2 &= \varkappa_1^1\varkappa_2^1(d_{21}^{11})^2 - (\varkappa_1^1 + \varkappa_2^1)M.
\end{aligned}$$

Further, we shall assume, that the vortices of the upper (lower) layer have a negative (positive) vorticity, i.e. $\varkappa_1^{1,2} = -\varkappa_2^{1,2} \equiv -\varkappa < 0$. Thus the relation $P = 0$ is equivalent to a condition of the central symmetry in vortex disposition on the plane, what, in particular, is confirmed by a new form of the equations (3):

$$\varkappa(d_{22}^{21})^2 = \varkappa(d_{11}^{21})^2 + 2M, \qquad (d_{21}^{22})^2 = (d_{21}^{11})^2, \qquad (d_{21}^{21})^2 = (d_{21}^{12})^2. \tag{3.1}$$

Let us consider now separately the cases of equality and inequality to zero of the moment M.

3.1. The case $M = 0$

The relations (3.1) allow to exclude one of the vortices, for example, the vortex with coordinates z_2^2, and to use trilinear coordinates (t_1, t_2, t_3) [18]:

$$t_1 = 3\varkappa(d_{21}^{12})^2, \qquad t_2 = 3\varkappa(d_{21}^{11})^2, \qquad t_3 = -3\varkappa(d_{11}^{21})^2, \tag{3.2}$$

moreover

$$t_1 + t_2 + t_3 = 0. \tag{3.3}$$

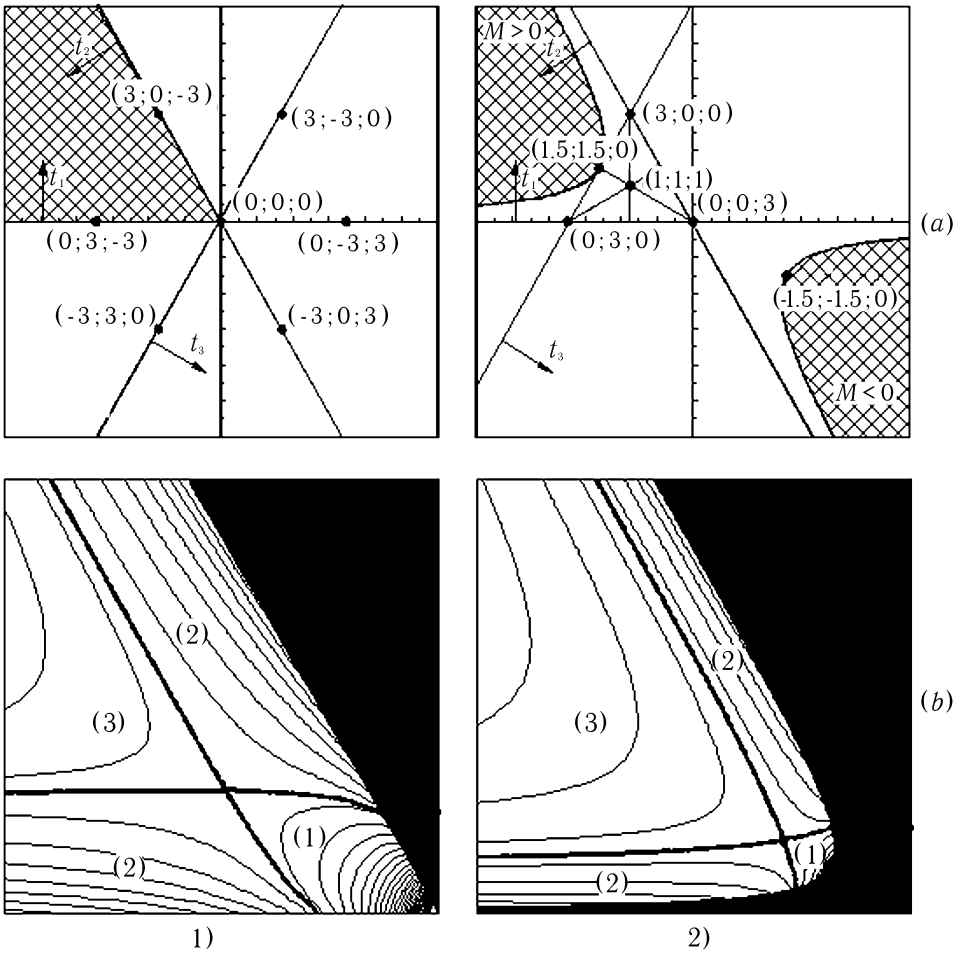

Fig. 1. (a) Trilinear coordinate system (t_1, t_2, t_3) with *physical areas* marked out by hatching for the cases: 1) $M = 0$, 2) $M \neq 0$;
(b) Phase portraits of the relative motion of the system in the trilinear coordinates: 1) $M = 0$, 2) $M > 0$

Trilinear axes of coordinates (3.2) are represented in a Figure 1.1 a, where the shading depicts *physical area*, in which the inequality of a triangle for distances d_{21}^{12}, d_{21}^{11}, d_{11}^{21} is fulfilled. In this case the boundary of the physical area is limited by straight lines

$$t_1 = 0 \qquad \text{and} \qquad t_2 = 0 \qquad \text{at} \qquad t_3 \leqslant 0. \tag{3.4}$$

Level curves of the Hamiltonian (2.4) will coincide with the level lines of the function

$$f(t_1,\, t_2) = \begin{cases} \ln\dfrac{t_1+t_2}{t_1 t_2} - 2\Big[K_0\Big(\gamma\sqrt{\dfrac{t_1+t_2}{3\varkappa}}\Big) + K_0\Big(\gamma\sqrt{\dfrac{t_1}{3\varkappa}}\Big) + K_0\Big(\gamma\sqrt{\dfrac{t_2}{3\varkappa}}\Big)\Big], & t_1,\, t_2 > 0, \\ -2\Big[\ln\dfrac{\gamma}{2} + C + 2K_0\Big(\gamma\sqrt{\dfrac{t_2\,(t_1)}{3\varkappa}}\Big)\Big], \quad t_1 = 0, \quad (t_2 = 0), \end{cases} \tag{3.5}$$

where $C \approx 0.5772$ is the Euler constant.

Hereinafter it is supposed, that the thicknesses of the upper and lower layers are equal: $h_1 = h_2 = 1/2$. The characteristic phase portrait is submitted in Figure 1.1 b. In it and in Figure 1.2 b the *nonphysical* part of the plane is black. The areas for three types of solutions can be specified by:

(1) — finite periodic motions;

(2) — infinite motions, during which the hetons run in opposite directions, remaining indivisible two-layer pairs;

(3) — infinite motions, when the hetons exchange the partners, and only then happens the scattering of newly formed two-layer pairs happens.

In the given special case ($M = 0$) the disposition of vortices submits to conditions of an additional symmetry with respect to both axes x and y. The motion of a representative point on a phase plane corresponds to the real motions of a system of vortices. The point which is coming nearer to the boundary of the physical area, "is reflected" from it and reverses its motion direction. Let us note two important singularities of distribution of phase curves:

1) For the first two types of motion the phase curves have the common points with the boundary line of the physical area (3.4);

2) All phase curves of the first and the third types intersect a straight line $t_1 = t_2$.

The first case describes a situation, when for both two-layer pairs the coordinates of the vortices in the upper and lower layers coincide (we observe two vortices with *vertical axes*). In the second case four elementary vortices are placed in angles of imaginary square. Hence, we can conclude, that it is possible to investigate completely all motions of a considered type if we assume, that in an initial moment:

(i) Each of two interacting hetons has *a vertical axis*,

(ii) All four vortices are located *in angles of some square.*

The solid curves on phase portraits represent separatrices, dividing the domains of the plane corresponding to various types of solutions. The coordinates of a point of self-intersection of a separatrix in Figure 1.1 b are defined by the requirement of the left-hand side in (2.1) to be equal to zero. Under the above conditions of the symmetry it reduces into a transcendental equation

$$\frac{1}{w} = 2\Big[K_1(w) + \frac{1}{\sqrt{2}} K_1(\sqrt{2}w)\Big] \tag{3.6}$$

where $w = \gamma d$, and d is a square side specified in the item (ii). The equation (3.6) has an approximate solution $w = w^* = 1.5947$. This point corresponds to the state, when the vortices located in the angles of the square occupy a stationary (unstable) position.

The phase trajectories for the case $M = 0$ can be investigated directly on the plane (x, y), without using trilinear coordinates. In particular, this is made in [8]. However, if a moment is not equal to zero, this approach gives a unique possibility for the qualitative analysis of the system.

3.2. The case $M \neq 0$

If $M \neq 0$, instead of (3.2) and (3.3) we have

$$t_1 = \frac{3\varkappa (d_{21}^{12})^2}{M}, \qquad t_2 = \frac{3\varkappa (d_{21}^{11})^2}{M}, \qquad t_3 = -\frac{3\varkappa (d_{11}^{21})^2}{M}, \tag{3.7}$$

and

$$t_1 + t_2 + t_3 = 3 \tag{3.8}$$

respectively.

The axes of this coordinate system form an equilateral triangle with a height equal to 3. The appropriate trilinear axes and the *physical area* are represented in Figure 1.2 a. The boundary of the physical area in this case represents a hyperbola

$$t_1 \cdot t_2 = \frac{9}{4}, \tag{3.9}$$

and level curves of a Hamiltonian will coincide with level lines of the function

$$f(t_1,\, t_2) = \ln\Big[\frac{|3 - t_1 - t_2||9 - t_1 - t_2|}{(t_1 t_2)^2}\Big] - 2\Big[2K_0\Big(\gamma\sqrt{\frac{t_1|M|}{3\varkappa}}\Big) + 2K_0\Big(\gamma\sqrt{\frac{t_2|M|}{3\varkappa}}\Big) + \\ + K_0\Big(\gamma\sqrt{\frac{|3 - t_1 - t_2||M|}{3\varkappa}}\Big) + K_0\Big(\gamma\sqrt{\frac{|9 - t_1 - t_2||M|}{3\varkappa}}\Big)\Big]. \tag{3.10}$$

The phase curves, characteristic for this case are represented in Figure 1.2 b. The labels (1), (2), (3) have the same sense, as in the previous case, but now each of these types of motion has only the central symmetry. It is important to note, that in this case the phase curves cannot reach the axes t_1 and t_2, which are asymptotes for the boundary of the physical area (3.9). Thus, if the representative point is on the boundary of the physical area, it corresponds to a disposition of all four vortices along one straight line, i. e. they form a collinear configuration [3]. If it belongs to a straight line $t_1 = t_2$, the vortices should be located in the angles of some diamond. Let us note, that this diamond cannot take square shape, that would correspond to the case $M = 0$ already considered.

Thus, now elementary cases of the initial disposition of the vortices designated for the previous case as (i) and (ii) take the following form:

(i) All four vortices form a *collinear configuration* with respect to some central point, thus a case $M > 0$ ($M < 0$) will correspond to such disposition, when the vortices of the lower (upper) layer are placed on edges, and vortices of the upper (lower) layer are placed inside the configuration;

(ii) The vortices are located *on two perpendicular straight lines*. At $M > 0$ the vortices of the lower (upper) layer lay on extremities of the longer (shorter) diagonal of the appropriate diamond, and at $M < 0$ the disposition of the vortices in the layers becomes opposite.

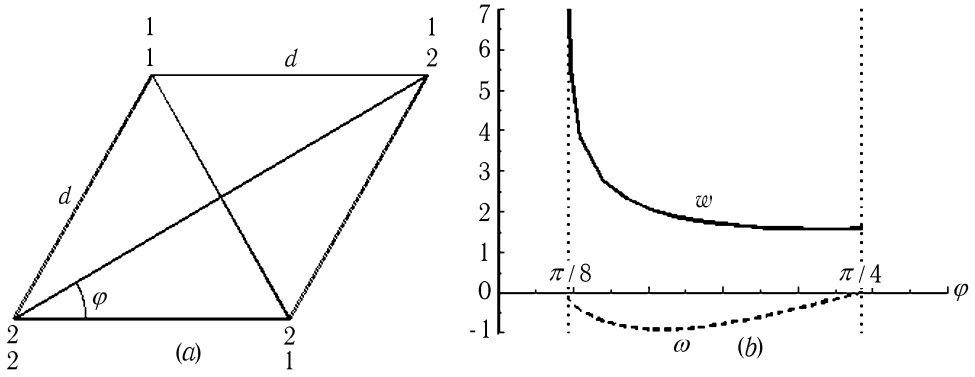

Fig. 2. (a) Scheme of instantaneous position of vortices during stationary rotational state (point of separatrix self-inersection);
(b) Functions $w(\varphi)$ marked by solid line, $\omega(\varphi)$ marked by dashed line at $M > 0$ given by the solutions of the equations (3.12) and (3.11) correspondingly

The point of self-intersection of a separatrix in this case corresponds to a stationary rotational state of the system made up of vortices located at the angles of a diamond. This rotation is directed

clockwise, if $M > 0$, and counter-clockwise, if $M < 0$. Designating the angular velocity of such rotation by ω, it is easy to set a condition that to the solution coresponds to the given state:

$$\omega = -\frac{\dot{x}_1^1}{y_1^1} = -\frac{\dot{x}_2^1}{y_2^1}. \tag{3.11}$$

From (3.11) we obtained the equation

$$8[1 - wK_1(w)] = \frac{1}{\sin^2\varphi}[1 + 2w\sin\varphi K_1(2w\sin\varphi)] + \frac{1}{\cos^2\varphi}[1 + 2w\cos\varphi K_1(2w\cos\varphi)], \tag{3.12}$$

where w has the same meaning, as in (3.6) with only difference, that now d is the length of the diamond side, and the meaning of an angle φ becomes clear from Figure 2 a. Obviously, at $\varphi = \pi/4$, the equation (3.12) takes the limiting form (3.6). It is easy to see, that the equation (3.12) is symmetric about $\varphi = \pi/4$. The case $M > 0$ corresponds to values $\varphi < \pi/4$, and the case $M < 0$ — to $\varphi > \pi/4$. Figure 2 b shows the distributions of the angular velocity (3.11), and also the solution of the equation (3.12) as function of the angle φ for the first of these cases. Obviously, at $\varphi = \pi/4$ we have $\omega = 0$. Let us note, that the limiting value of the angle of diagonal tilt is the value $\pi/8$, at which the length of the diamond side governed by equation (3.12), grows unrestrictedly, and the angular velocity tends to zero. Really, at $w \gg 1$ it is possible to neglect the terms containing modified Bessel functions. Then the remaining terms of (3.12) give the equation

$$\frac{1}{\sin^2 2\varphi} = 2$$

with obvious solutions $\varphi = \pi/8$ at $M > 0$ and $\varphi = 3\pi/8$ at $M < 0$. We obtain from (3.11)

$$\omega = \frac{\varkappa}{2\pi w}\Big(1 - \frac{1}{4\sin^2\varphi}\Big).$$

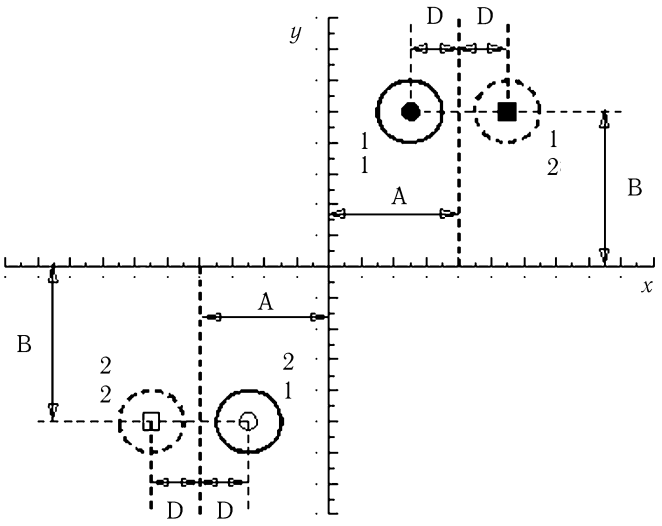

Fig. 3. Initial position of the vortices for the case of off-center collision of the hetons at $M > 0$

It is easy to see, that $\omega \to 0_-$ when $M > 0$, and $\omega \to 0_+$ when $M < 0$. Thus, the stationary solutions of this type exist only in area $|\pi/4 - \varphi| < \pi/8$.

In the following section we still repeatedly shall refer to results of the phase curve's analysis.

4. Analysis of absolute motion

Above it was noted, that for obtaining a comprehensive idea of two heton interaction it is enough to consider cases of an initial disposition of vortices specified in (i) and (ii). Nevertheless, having in view most interesting applications to hydrodynamic problems, we shall consider such variants of the initial disposition of vortices (Figure 3), at which the proper motion of each of two-layer pairs initiates their head-on collision. In this Figure the two-layer vortex of the upper half-plane has number 1, and lower half-plane — number 2. As well as in the formulas (2.1) the superscript corresponds to the heton number, and subscript corresponds to the layer number. The value $2D$ that is equal to a distance between the upper and lower vortices in each heton, characterizes a "tilt" of the heton's axis, and $2A$ and $2B$ represent distances between "centers of vorticity" of the first and the second hetons along the axes x and y respectively. The circle solid (empty) markers designate the location of vortices in the upper layer, and box ones designate the locations in lower layer for the first (second) heton. The same labels take place in the consequent figures, where the larger markers correspond to initial positions of the vortices. It is clear, that $M = 0$ corresponds to the case $A = 0$. Having such initial position the hetons participate in the motion which results in a head-on collision. At $A \neq 0$, i. e. $M \neq 0$, their position promotes the motion of each of the two-layer pairs along antiparallel rays (off-center collision) carried on a distance $2A$.

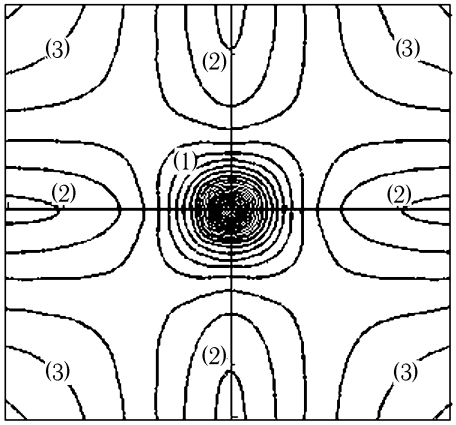

Fig. 4. Isolines of the Hamiltonian (2.4) in rectangular coordinates $(\gamma x, \gamma y)$ at $h_1 = h_2 = 1/2$ and $M = 0$

The numerical solution of a system of the ordinary nonlinear differential equations (2.1) was carried out using of the second-order Runge–Kutta scheme with time step $\triangle t = 0.01$. The initial conditions are completely defined by setting values of the parameters A, B and D. The rotational period of a liquid particle put away from the point vortex because unit distance was chosen as a dimensionless time unit; the distance is normalized by the Rossby radius of deformation λ.

4.1. The case $M = 0$ $(A = 0)$

Here we shall touch on this question briefly, as it is investigated completely enough in [8]. As it was mentioned above, at $M = 0$ the study of a phase curve behavior is also possible on a plane $(x,\ y)$, that is confirmed by Figure 4. During a head-on two heton collision the types of motion (1)–(3) take the following form:

(1) Anticyclonic (cyclonic) rotation of vortices in the upper (lower) layer along closed "O-shaped" [8] mutually covering trajectories;

(2) Rapprochement of hetons at which the change of the tilt sign of their axes happens, they turn by 180° and scatter in opposite directions;

(3) Rapprochement of hetons when each of four vortices turns by 90°, they interchange the partners, and newly formed pairs scatter in opposite directions.

Obviously, the trajectories have a finite character of the first type of motion, and in case of the second and third ones they have the infinite characters. The motion of the types (2) and (3) has basically baroclinic nature, as here the interaction of the vortices from different layers is predominant. In the case (2), during evolution, each of the hetons remains indivisible two-layer dipole, while in the case (3) the hetons exchange the partners, the topology of the stream functions for motion of a last type being the same as for the point vortices in a homogeneous liquid [13]. For the motion of the type (1), on the contrary, the barotropic (intralayer) character of interaction evidently predominates.

Here the baroclinic mechanism becomes apparent only due to the deviation of the closed trajectory's shape from circular[1]. In the case of the two-layer liquid the closed trajectories tend to take the form, close to circular at $w \to 0$, and the form of the deformed square at $w \to w^*$, where w^* is the solution of the equation (3.6). Moreover, at $w \to w^*$ the velocity of vortex rotation becomes more and more non-uniform, as the angular points are the points of vortex stagnation.

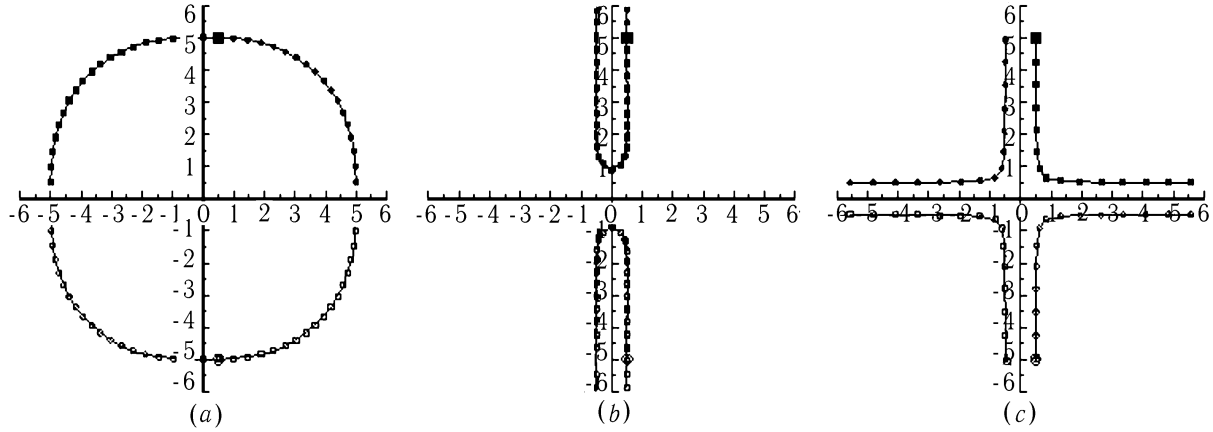

Fig. 5. Point vortex trajectories at $A = 0$, $B = 5$, $D = 0.5$: (a) $\gamma = 0.1$, (b) $\gamma = 1.0$, (c) $\gamma = 2.0$.

The examples of trajectories of vortex motion for all three types are shown in Figure 5. Here and in majority of similar figures the vortex trajectories are drawn as continuous lines with markers, plotted with regular time interval. And, we shall remind, the larger markers indicate initial coordinates of the vortices. For all three cases the initial position of the vortices is the same. The passage from one type of motion to another is stipulated only by modifications of a parameter γ. It happens as follows. Let, in the initial moment, a point in a phase space has a fixed coordinates (x, y), and at the given value γ it founds itself in the area (1). The growth of the parameter γ brings to the reapproching of the boundaries of the areas (3) due to the compression of areas (1) and (2). In this case, if the point does not belong to straight lines $y = \pm x$, $y = 0$ or $x = 0$, it will belong sequentially to the areas (1), (2), (3), if γ will grow. This is confirmed also by the series of Figures 5 a, 5 b, 5 c.

In all fragments of the figure, only the initial stages of the motion are shown. In particular, in Figure 5 a each vortex pass about a quarter of its cyclic orbit during the time of calculation. The consequent evolution of the vortex system is not represented here in order to avoid the overloading of the Figure. We can see, that the vortices of the upper layer move anticyclonically, and the vortices of the lower layer — in the opposite direction.

In Figure 5 b, at the initial stage of evolution, both pairs move towards each other. Closer they approach, the stronger becomes the interference of vortices inside each layer, this effect adds the rotary component of motion to the translation one. As a result, axis tilt of each heton decreases, hence, the translation velocity decreases (vanishing, if the angle of the axis tilt becomes zero). Further, in each of the hetons the vortices of the upper and lower layers interchange their position (in a horizontal plane), i. e. the axes change signs of their tilt, hence the hetons change the direction of their motion to the opposite one. No real collision of the hetons occur; "interheton repulsion" takes place over a distance. It reminds a problem on two balls, when their opposite motion during the time interval of one oscillation is initiated by springs attached to them and initially compressed.

The experiment, illustrated by Figure 5 c, gives an example of the type (3) motion, when the interaction between vortices of opposite layers predominates during all stages of the process.

[1]It is known (see, for example, [13, 12]), that two identical votrices in a homogeneous liquid rotate on the circular orbit around their geometric center with constant angular velocity.

4.2. The case $M > 0$ $(A > 0)$

Let us consider peculiarities of two-heton interaction during their off-center collision. In addition to phase curves (Figure 1.2 b) we would like to show the existence domains of various types of absolute motion in the space of exterior parameters (γ, A, B, D), obtained by numerical experiments. The appropriate diagrams as the several sections of this space by a plane (γ, A) are given in Figure 6. It is important to note, that, besides the types (1)–(3) of the motion mentioned above, we observed one new, type — (1*), which, at first, is possible only at $A \neq 0$, and, second, does not appear on the phase portrait constructed for relative motions (Figure 1.2 b). The peculiarities of this class of motions are discussed below.

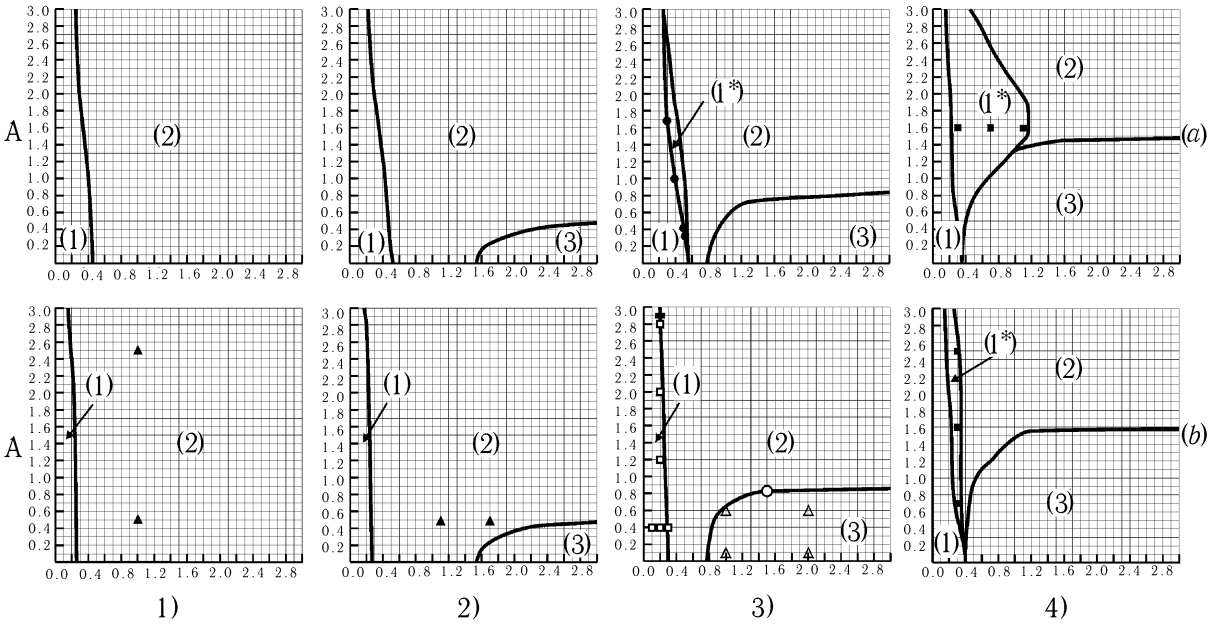

Fig. 6. Diagrams of existance domains for different types of solutions for the absolute motion of two-heton system in the first quadrant of the plane of parameters (γ, A) at:
(a) $B = 1.5$, (b) $B = 2.5$;
1) $D = 0.2$, 2) $D = 0.5$, 3) $D = 1.0$, 4) $D = 2.0$.
Markers in the Figure correspond to the external parameters used in numerical simulations demonstrated by Figures 7–13, 15

4.2.1. The types (2) and (3)

At the stage of running away the trajectories of the vortices taking part in the infinite motions have turning angles, depending on the parameter A with respect to the direction of their initial motion which are not equal to 180° and 90° angle α (Figure 7) for the motions of type (2), and angle β (Figure 8) for type (3) correspondingly[2]. Both Figures demonstrate the degree of influence of parameters A and γ on the character of vortex motion.

Figure 7 a demonstrates fairly obvious effect: the growth of the parameter A is accompanied by growth of the angle α. Really, it is clear, that if the hetons are carried far enough (large values of A), they should move rectilinearly, practically "not feeling" each other. According to Figure 7 b, the similar result has a place when the parameter of stratification γ increases, since the interaction between the vortices from different layers becomes stronger.

[2]More precisely speaking, the angles α and β characterize clockwise deviation of trajectories of the vortex with indexes $\binom{1}{2}$ from the appropriate direction at $A = 0$.

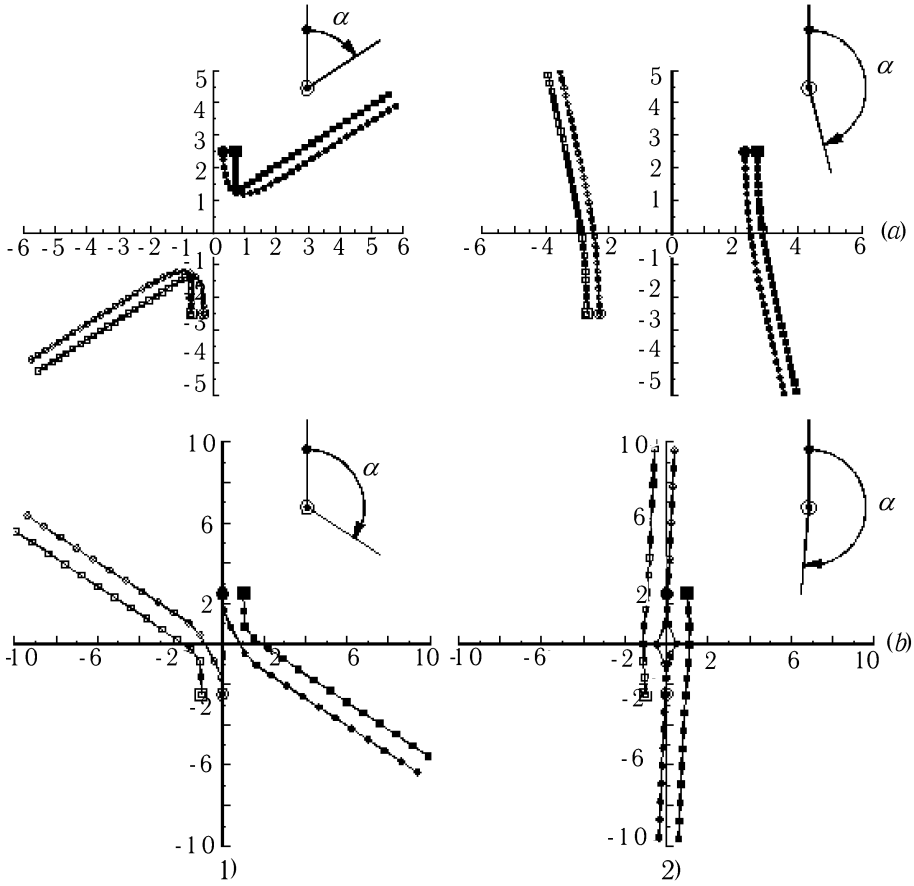

Fig. 7. Trajectories of point vortices at $B = 2.5$:
(a) $D = 0.2$ $\gamma = 1.0$; 1) $A = 0.5$, 2) $A = 2.5$;
(b) $D = 0.5$, $A = 0.5$; 1) $\gamma = 1.1$, 2) $\gamma = 1.7$.
(Black triangles in Fig. 6.1 b and 6.2 b correspond to the initial position of the vortices)

In Figure 8 the role of the same parameters for motions of the type (3) is shown. In Figure 8 a, the influence of a parameter γ is almost not felt. In this case it is explained by a smallness of the parameter A, as at $A = 0$ the angle becomes $\beta = 0$. At the greater value of a parameter of asymmetry A (Figure 8 b) we again can state, that the growth of γ promotes the intensification of the interlayer interaction.

It is interesting to note two basically different cases (Figure 7.2 b and Figure 8.1 b). In first of them, belonging to the type (2), the vortices of the upper layer, practically not "seeing" each other, still move in the initial direction accompanied by their partners from the lower layer. In the second case, on the contrary, each of them, approaching the "adversary" at some distance, swings around, and, further, moves in the opposite direction together with the vortex of the upper layer initially belonging to the other heton.

In a vicinity of the boundary dividing areas (2) and (3) in the space of exterior parameters, transfer from one type of motion to another occurs, that is demonstrated in fragments 1) and 2) in Figure 9, where the values of parameter A values differ only by 10^{-5}. We can see, that at the intermediate stage of interaction the vortices of both hetons in the upper layer "try" to pass to quasi-circular trajectories, but then fell down, and run away, either staying a heton (type (2), case 1 a), or, making made the exchange of the partners (type (3), case 2 a). Let us note, that in Figure 9.1 a the angle α exceeds 450°. On a phase plane (Figure 9 b), the marked points corresponding to the initial state of the system, visually are indiscernible and, practically, lay on a separatrix. Obviously, at the

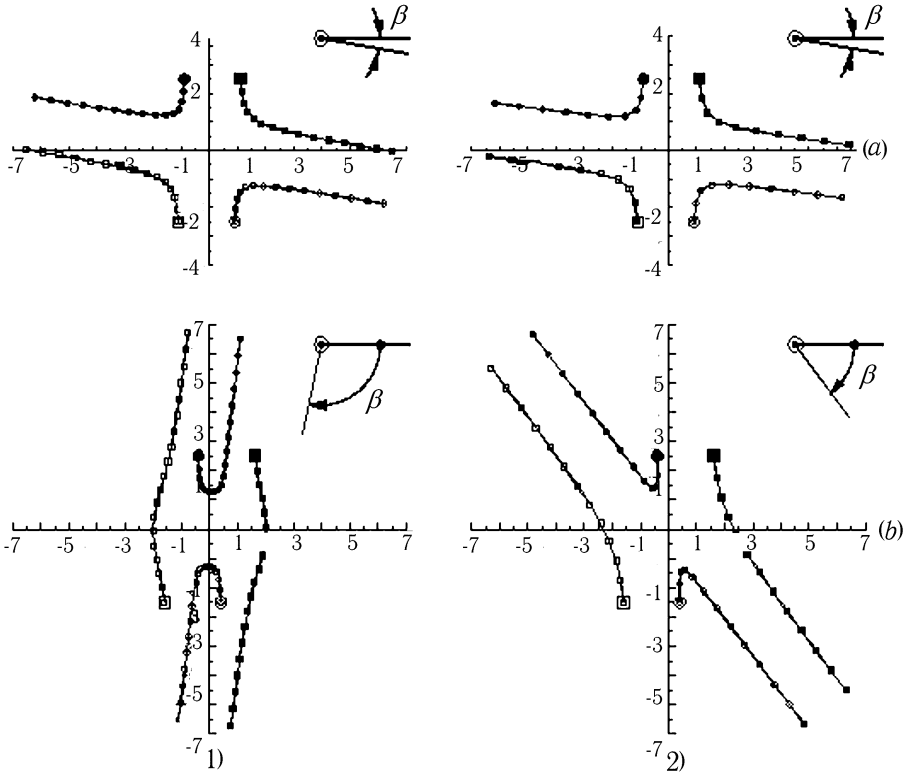

Fig. 8. Trajectories of point vortices at $B = 2.5$, $D = 1.0$:
(a) $A = 0.1$, (b) $A = 0.6$;
1) $\gamma = 1.0$, 2) $\gamma = 2.0$.
(Empty triangles in Fig. 6.3 b correspond to the initial position of the vortices)

stage of the quasi-circular vortex rotation, the representing points are in the vicinity of the point of self-intersection of the separatrix.

4.2.2. The types (1) and (1*)

If at $A = 0$, in the case of motions of the type (1), the vortices of the upper and lower layers moved in opposite directions but along the same trajectories, now the behavior of the vortices in different layers has the qualitative differences. Moreover, at $A \neq 0$ one more type of interaction (1*) appears: the vortices of both layers perform rotations, localized inside some limited area, in the same direction, and not in the opposite directions, what is characteristic for the type (1).

Results of the study of the finite type interaction are submitted below. To identify the figures, only the initial positions of vortices are shown in the subsequent illustrations.

Figure 10 displays motion peculiarities for the type (1) as function of external parameter variation. The upper row of the Figure 10 a shows that the growth of the stratification parameter γ promotes the amplification of dispersion properties of the vortex trajectories: in addition to azimuth rotation along closed quasi-circular curves, the vortices get nutational components. It has the following physical explanation. Small values of γ correspond to large jumps of density at the interface of the layers, that hinders the interaction between vortices of different layers; that's why their trajectories are practically circular (quasi-barotropic behavior); see as example Figure 10.1. As it was mentioned above, if γ is growing, the intralayer interaction of the vortices increases. The latter promotes the tendency of the vortices to fall down from circular orbits, and pass to the motions of the infinite type. The lower row

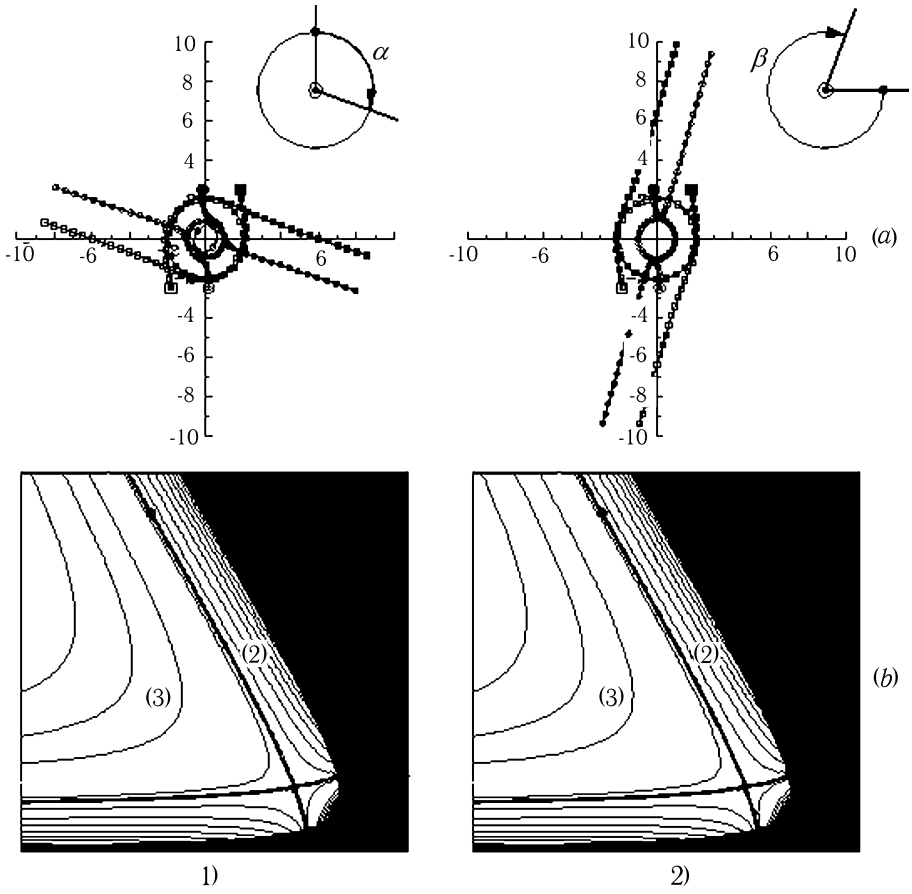

Fig. 9. (a) Trajectories of point vortices at $B = 2.5$, $D = 1.0$, $\gamma = 1.5$: 1) $A = 0.83170$, 2) $A = 83169$;
(b) Corresponding phase portraits.
(Empty circle in Fig. 6.3 b corresponds to the initial position of the vortices)

of the Figure illustrates the influence of the parameter A on the interaction character of the system of two-layer vortices. One can see, that the growth of the parameter of asymmetry calls:

- The difference in the absolute values of the angular velocity of the orbital motion in different layers increases: in the lower layer the module of the angular velocity noticeably decreases. There is a simple explanation to this phenomenon. As the vortices of the lower layer become more distant one from other (with growth of A), and their interaction, that initiates rotation in the cyclonic direction, weakens, they experience the more powerful influence from the anticyclonically curled upper layer vortices that are located closer with each other.

- Growth of nutational motions in the lower layer also due to the stronger influence of the vortices of the upper layer.

- Relative ordering of the vortex trajectory's behavior in the upper layer. As it will be shown below, this phenomenon is connected with the fact that with the growth of A in the given series of experiments, we come nearer to the boundary of existence domain of the solutions of the given type.

The last statement is demonstrated, in particular, by Figure 11, where the behavior of a system of interacting vortices in a neighborhood of the boundary between areas (1) and (2) is shown. The exterior parameters for all experiments here differ so unsignificantly, that only one marker corresponds

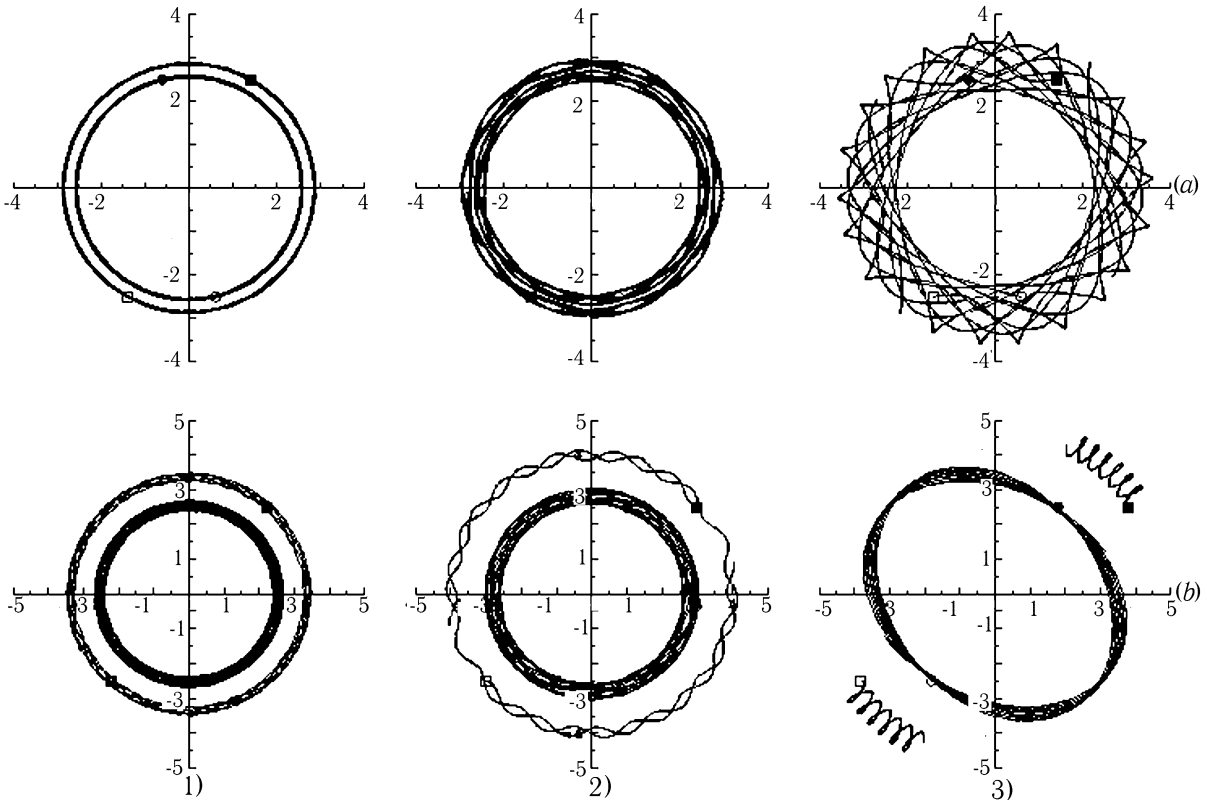

Fig. 10. Trajectories of point vortices at $B = 2.5$, $D = 1.0$:
(a) $A = 0.4$; 1) $\gamma = 0.1$, 2) $\gamma = 0.2$, 3) $\gamma = 0.3$;
(b) $\gamma = 0.2$; 1) $A = 1.2$, 2) $A = 2.0$, 3) $A = 2.8$.
(Empty boxes in Fig. 6.3 b correspond to the initial position of the vortices)

to them in the plane (γ, A). Moreover, here we observe examples of type 1^* motion, which are not shown at all in the Diagram 6.3 b: it is connected to the fact that the existence domain of the appropriate type motion is so narrow, that it is taken up by a thickness of the boundary line between areas (1) and (2). Each of the raws (a), (b), (c) illustrates the change of regimes with weak growth of the stratification parameter. So, in Figures 11 a and 11 c we observe passages (1) $\to$ (1^*) $\to$ (2) and (1) $\to$ (1^*) correspondingly. If for the case of the type (1) motions we designate by T_t, T_b the rotation periods of the upper and lower layer vortices in the anticyclonic and cyclonic directions respectively, and by t_b the period of nutational oscillations of the lower layer vortices, the analysis of calculation results shows that we have the following relationships in a neighborhood of the boundary between the regimes (1) and (1^*):

$$\frac{T_t}{T_b} \to 0, \tag{4.1}$$

$$\frac{T_t}{t_b} \to 2. \tag{4.2}$$

As to Figure 11 b, besides the motions of types (1) and (2) we have here a possibility to observe the realization of an intermediate stationary condition (Figure 11.2 b) with the following properties:

a) The vortices of the upper layer perform only periodic rotations along trajectories of the quasi-elliptical form.

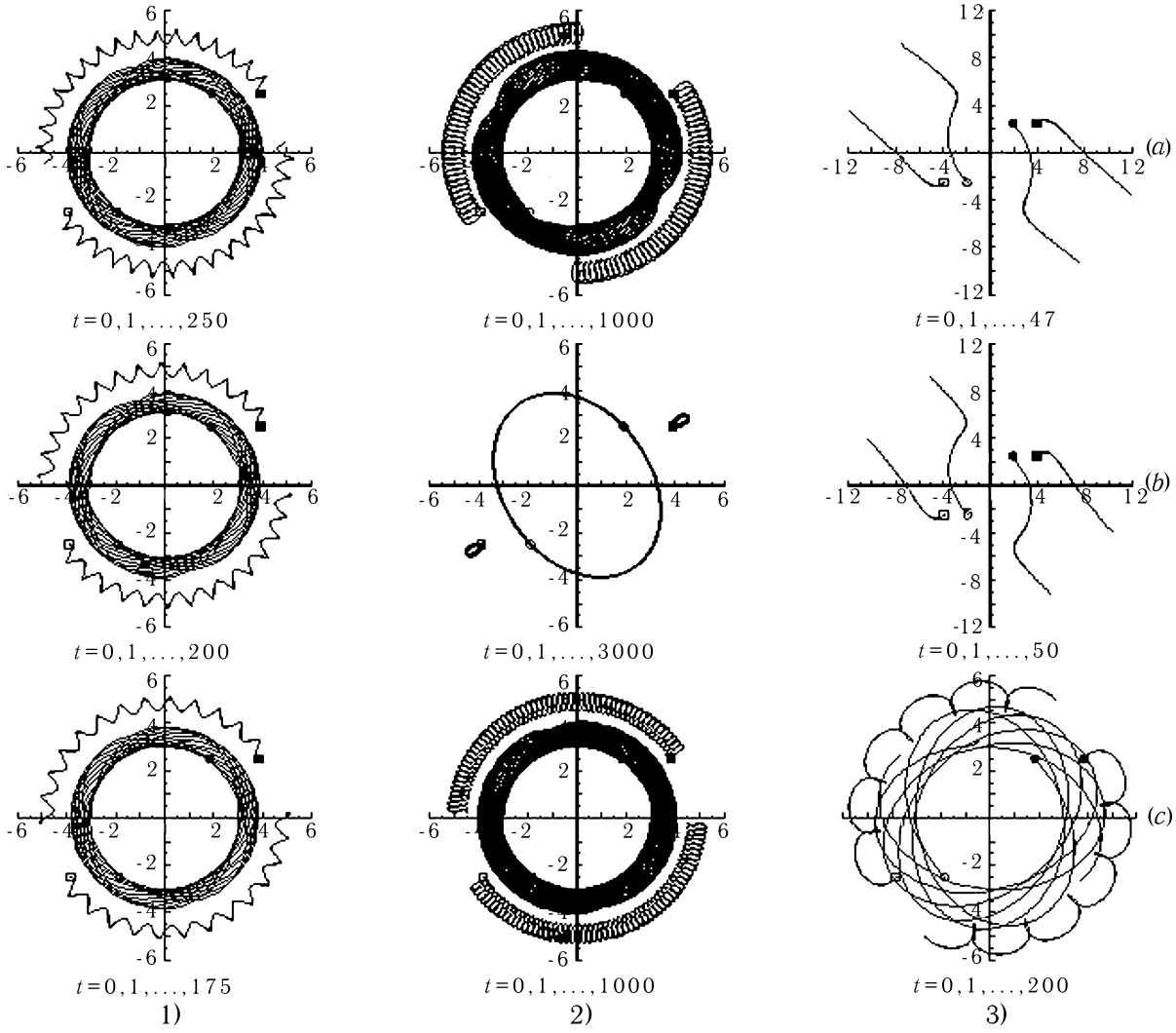

Fig. 11. Trajectories of point vortices at $B = 2.5$, $D = 1.0$:
(a) $A = 2.94$, (b) $A = 2.89845$, (c) $A = 2.85$;
1) $\gamma = 0.19$, 2) $\gamma = 0.20$, 3) $\gamma = 0.21$.
(Black rectangle in Fig. 6.3 b corresponds to the initial position of the vortices)

b) The vortices of the lower layer perform periodic nutational rotations around some motionless points. It that hapens, it appears, that in relations (4.1) and (4.2) the limit values 0 and 2 correspondingly are reached.

In this Figure the integration time of the appropriate calculation are indicated under each of the fragments. The large integration time in Figure 11.2 b affords ground to suppose that this stationary solution is steady. This fact, in particular, confirms the property formulated in item b) stating that for the given solution $T_t/T_b = 0$.

Let us formulate the following *hypothesis*:

> Under certain relations between exterior parameters of the problem the anticyclonic vortices of the upper layer move periodically along such closed quasi-elliptic figure, that at its periphery stipulates the presence of two stationary points, located in the lower layer.

The validity of a limit relation in (4.2), namely, $T_t/t_b = 2$, is demonstrated in Figure 12, where the values of exterior parameters are the same, as in Figure 11.1 b.

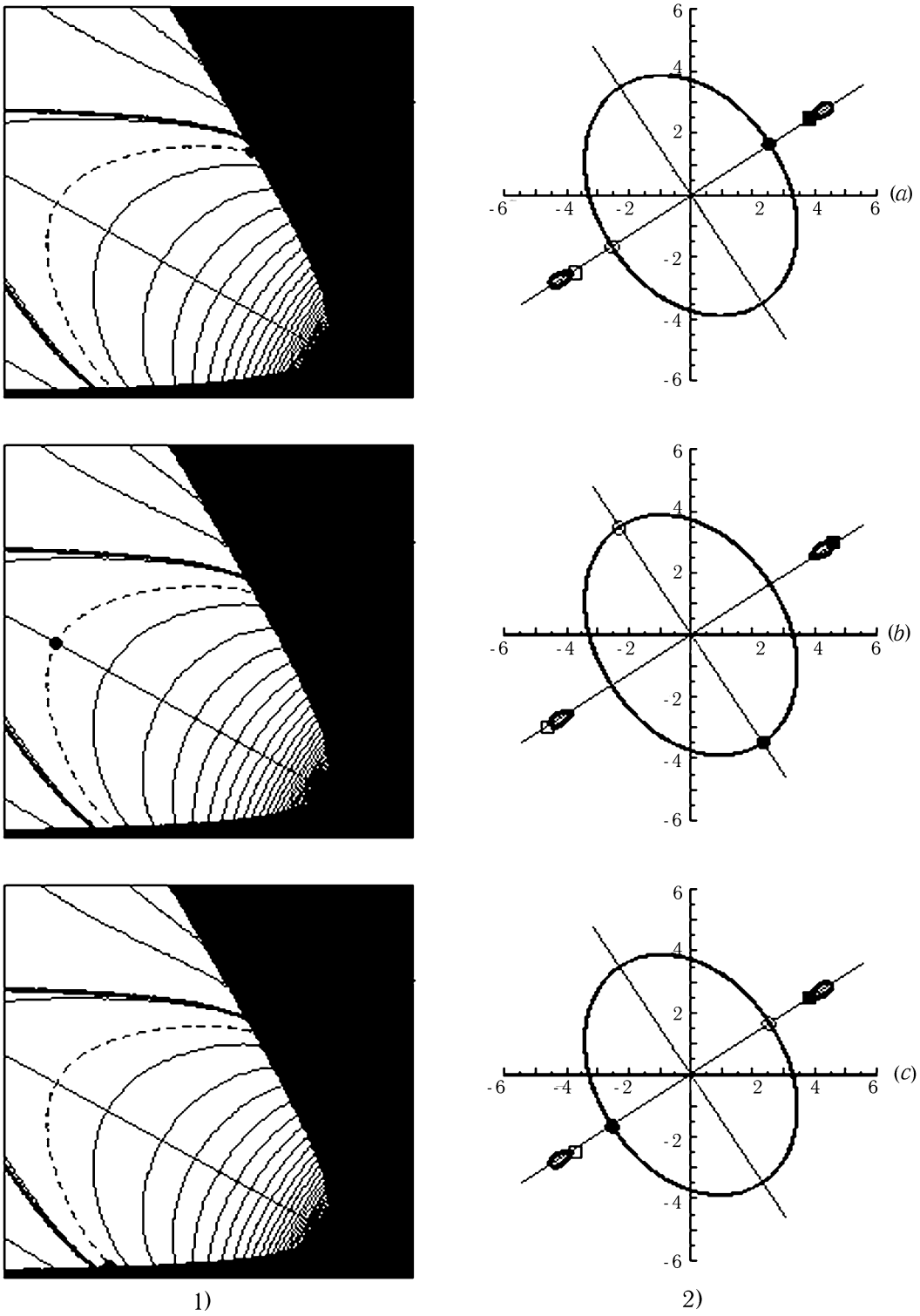

Fig. 12. Instantaneous positions (at $A = 2.89845$, $B = 2.5$, $D = 1.0$, $\gamma = 0.2$) of
1) representing point on the phase plane,
2) vortices into their trajectories in moments:
(a) $t = t^*$, (b) $t = t^* + T_t/4$, (c) $t = t^* + T_t/2$,
where t^* — any moment, when the vortices form a collinear configuration

In the phase space (Figure 12.1) the straight line is defined by the equation $t_1 = t_2$, and the dashed line represents a trajectory of a characteristic point of the given numerical experiment. Positions of the characteristic point indicated by black circles, and corresponding coordinates of vortices marked in the adjacent fragments of Figure 12.2 were made after the analysis of the expression for the Hamiltonian (3.6). The sequence of rows $12\,a \to 12\,b \to 12\,c$ covers the interval equal to a full period (half-period) of evolution of the vortices of the lower (upper) layer along their trajectory. Thus, it becomes clear, that the period ratio T_t and t_b is equal to 2.

A series of configurations of similar type is given in Figure 13, where the parameters γ and A belong to the interface between areas (1) and (1*). As we can see, if A is growing, the amplitude of nutational oscillations of the lower layer vortices decreases, and, thus, in the class of these intermediate motions it is possible to specify a subclass, corresponding to the solutions which describe the anticyclones of the upper layer moving along the cyclic orbit and motionless cyclones of the lower layer. In this Figure the fragments (b) and (d) are supplied with the explanations in the form of phase portraits, where the point corresponds to the initial position of the vortex system. We can see, that in the case (b) the phase trajectory of a characteristic point has rather large span in the direction of the axis t_3, and in the case (c) — it is much smaller. It is explained by the fact that in the second case the trajectory of the upper layer vortices is less elongated (if it had the purely circular form, the corresponding phase curve would represent a segment, perpendicular to the axis t_3).

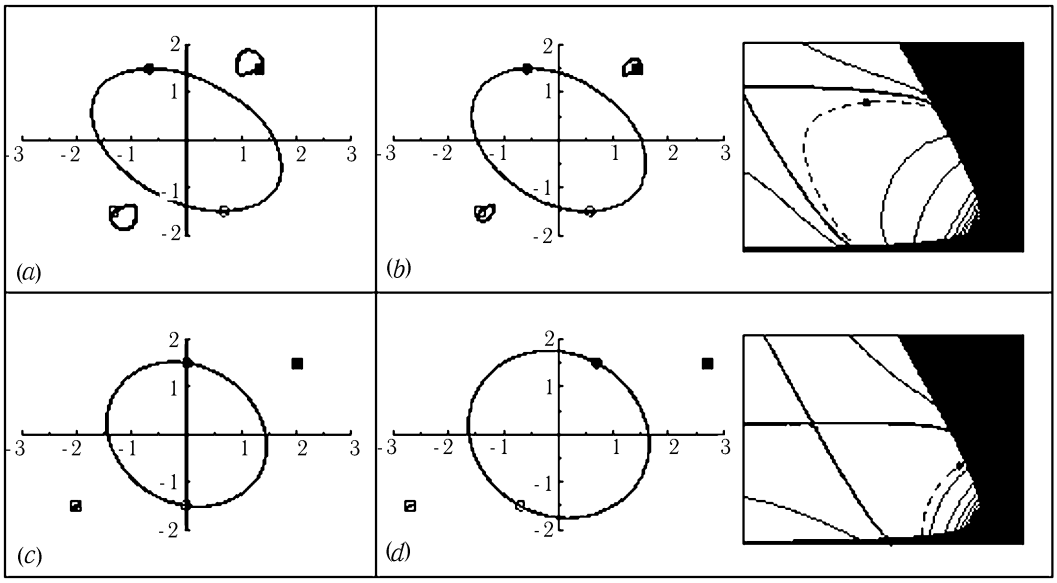

Fig. 13. Trajectories of vortices — (a) and (c), and their trajectories together with phase portraits — (b) and (d) (the representing point position corresponds to the initial configuration of the vortices) — at $B = 1.5$, $D = 1.0$:
(a) $A = 0.32367$, $\gamma = 0.52$, (b) $A = 0.42833$, $\gamma = 0.50$,
(c) $A = 1.00715$, $\gamma = 0.38$, (d) $A = 1.69710$, $\gamma = 0.30$.
(Black circles in Fig. 6.3 a correspond to the initial position of the vortices)

The example of a solution of the same type is given in Figure 14 a, where the duration of the computation, as well as in Figure 11.2 b, is defined by the interval $t = 0 \div 3000$. In our opinion, Figure 14 b argues in favor of the statement about stationarity of the given solution. The isolines of the Hamiltonian (2.4) for the problem on free anticyclonic vortex motion in the upper layer satisfying to the condition of the central symmetry and situated in the field of *motionless* (artificially fixed) cyclones of the lower layer. In this case, obviously, the isolines of the Hamiltonian coinciding with streamlines of the horizontal motion in the upper layer, can be represented on a plane of variables (x, y). As Figure 14 b shows, the vortices of the upper layer can perform motions of three types:

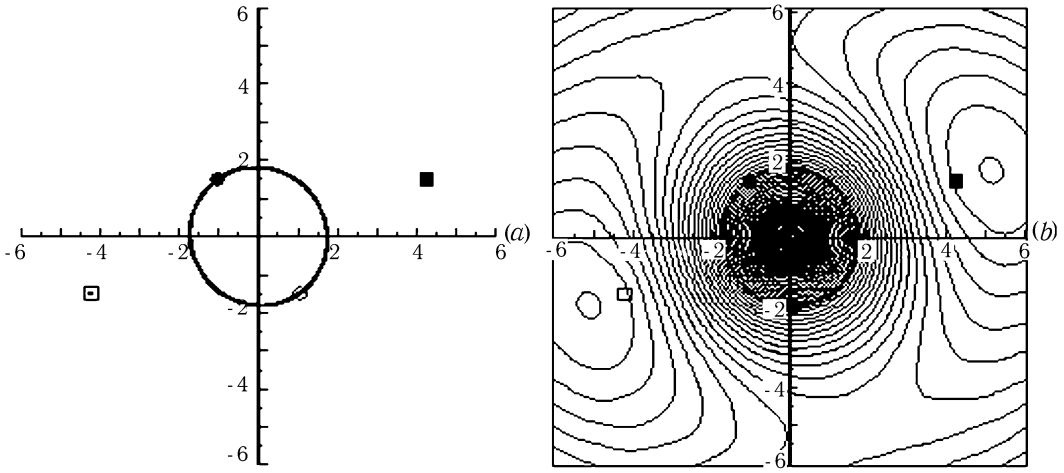

Fig. 14. Trajectories of point vortices — (a), and the phase portrait on the (x, y)-plane — (b) at $A = 1.6$, $B = 1.5$, $D = 2.642$, $\gamma = 0.2$. In the fragment (b) $x_2^1 = -x_2^2 \equiv A + D$, $y_2^1 = -y_2^2 \equiv B$

a) Separate cyclonic rotations around motionless vortices of the lower layer;

b) Anticyclonic rotation along common trajectories in the area located between the vortices of the lower layer;

c) Cyclonic rotation along trajectories enclosing area, where the vortices of the lower layer are concentrated; the last are seen by the vortices of the upper layer as one cyclonic formation.

Of course, the problem if Figure 14 b is a totally different problem from these of Figure 14 a. But in the space of initial parameters these two problems overlay, if the initial coordinates of all vortices coincide. The appropriate (zero-value) streamline in Figure 14 b is represented by a thick solid curve. The comparison shows, that it coincides with the trajectory of the upper layer vortices in Figure 14 a. As it is known from hydrodynamics, *the coincidence of the trajectory and the streamline is possible only in the stationary case*. Thus, there are grounds to suppose, that the solution given in Figure 14 a, determines a stationary state of the system consisting of two hetons.

Apparently, the last statement is valid for all solutions, if the parameters that correspond to them, belong to the boundary of the existence domains for the solutions of types (1) and (1*). This is valid, in particular, for solutions given in Figure 13.

Figure 15, by analogy to Figure 10, demonstrates how the character of the type (1*) motion is governed by parameters γ and A. In this case all four vortices move clockwise along the trajectories. For all six variants the computation time is approximately equal to the period of the rotation of the lower layer vortices along their trajectories.

Figure 15 a shows that the influence of the stratification parameter γ on solutions of this type, is not so significant, as for the motion of the type (1). Now the growth of γ (weakening of stratification) mainly increases dispersive properties of the trajectories in the upper layer, and affect rather weakly the behavior of the lower layer vortices. The analysis of solutions for the experiments 1), 2) and 3), given in Figure 15 b, reveals the growth of the ratio of rotation periods T_t/T_b, if the label T_b is applied now to the rotation period of the lower layer vortices in the anticyclonic direction. It becomes clear from the position of markers in Figure 6.4 b: if the parameter A grows sequentially and the passage $(15.1\,b) \to (15.2\,b) \to (15.3\,b)$ takes place, the appropriate point of the plane (γ, A) takes itself off the boundary of the areas (1) and (1*) and comes nearer to the boundary between the areas (1*) and (2).

Note, that some special cases of the heton off-center collision are studied also in the work [8, Figure 10].

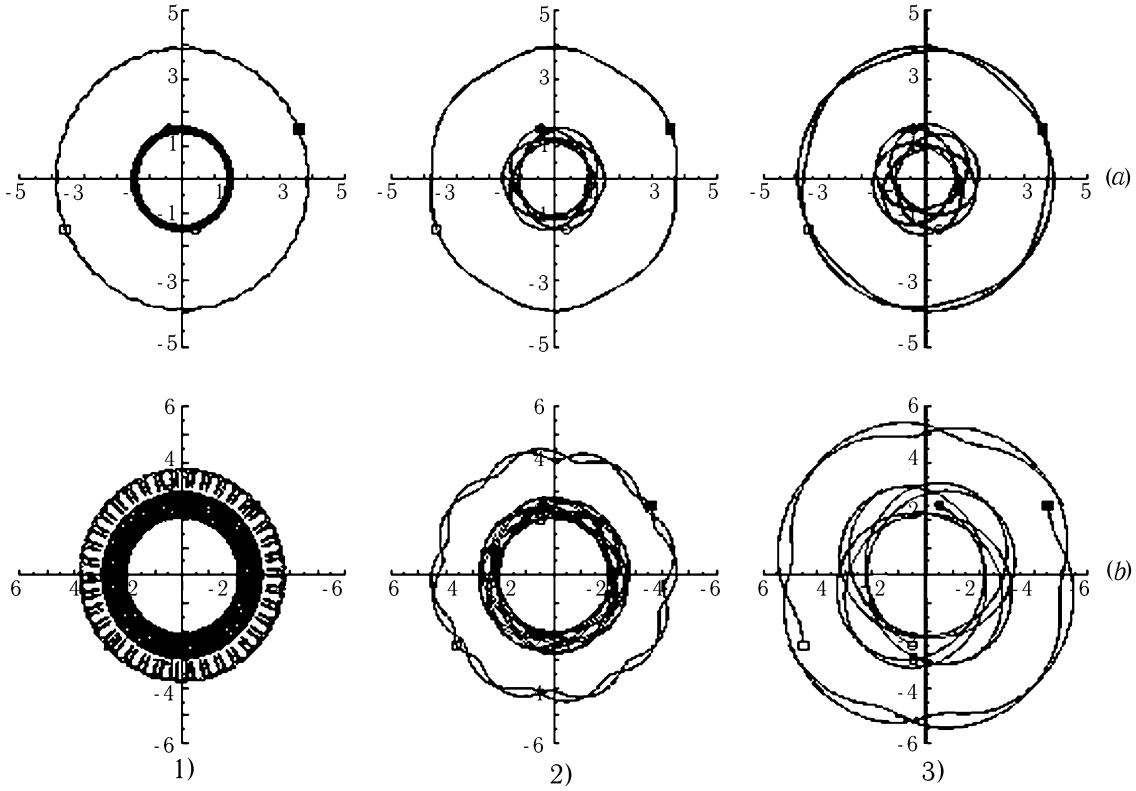

Fig. 15. Trajectories of point vortices at $D = 2.0$:
(a) $A = 1.6$, $B = 1.5$: 1) $\gamma = 0.3$, 2) $\gamma = 0.7$, 3) $\gamma = 1.1$;
(b) $B = 2.5$, $\gamma = 0.3$: 1) $A = 0.7$, 2) $A = 1.6$, 3) $A = 2.5$.
(Black boxes in Fig. 6.4a and 6.4b correspond to the initial position of the vortices)

5. Conclusion

The interaction of two compensated discrete two-layer vortices (hetons) with zero summarized impulse has been studied. The use of the Hamilton approach has allowed to make a conclusion about integrability of the initial system of differential equations for vortex motion. The qualitative analysis of relative vortex motion has been carried out. Series of numerical experiments allowed to investigate features of the absolute motion for the specific case of two heton off-center collision. Diagrams of possible types of motion in the space of the external parameters, defining the initial reciprocal position of vortices and the degree of stratification of a two-layer liquid have been constructed. It has been shown, that, unlike the case of a head-on collision of the hetons [8], a new type of finite motion is possible, when the vortices in both layers can rotate not only in opposite directions, but also in the same direction. The role of external parameters in forming peculiarities of various types of vortex motion has been investigated. A new type of an intermediate isolated steady stationary state has been found out, when the vortices in one of the layers perform periodic rotation motions, while the vortices in the second layer either perform periodic nutational oscillations around some peripheral motionless points, or, in the special case, hold stationary position in these points. Under small modifications of exterior parameters this solution bifurcates to one of the next states.

Let us remind, that in this work all calculations were carried out for the layers having equal thickness. In this case the layers are equivalent, so all the conclusions concerning the behavior of the vortices in any layer can be reformulated for the other one, if we change the sign of rotation of each vortex to the opposite one. If the layers have different thickness, but the compensation

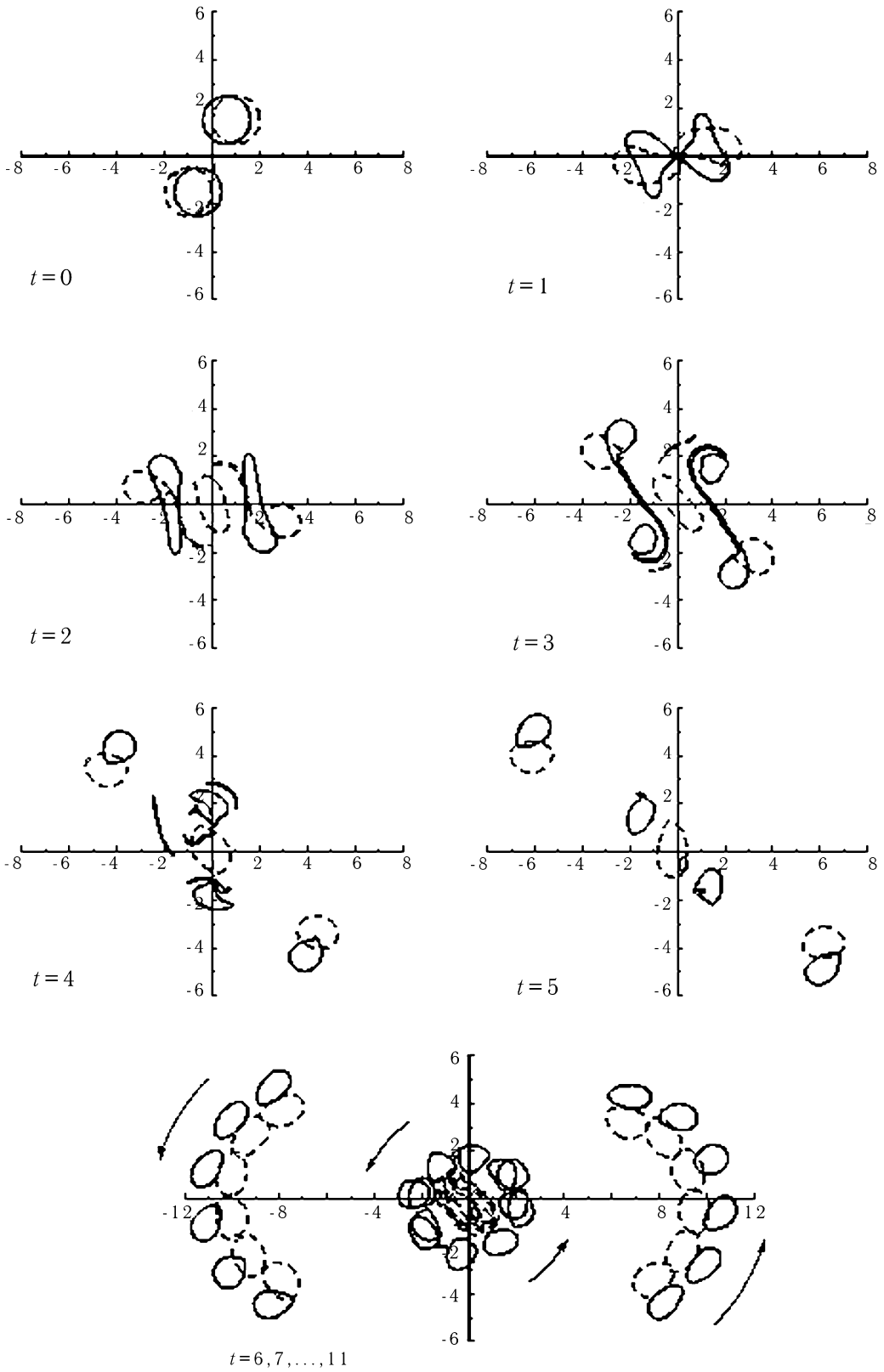

Fig. 16. Instantaneous configurations of vortex patches in the upper layer (solid lines) and lower layer (dashed lines) which form the hetons at $A = 0.8$, $B = 1.5$, $D = 0.2$, $\gamma = 2.0$ in indicated time moments

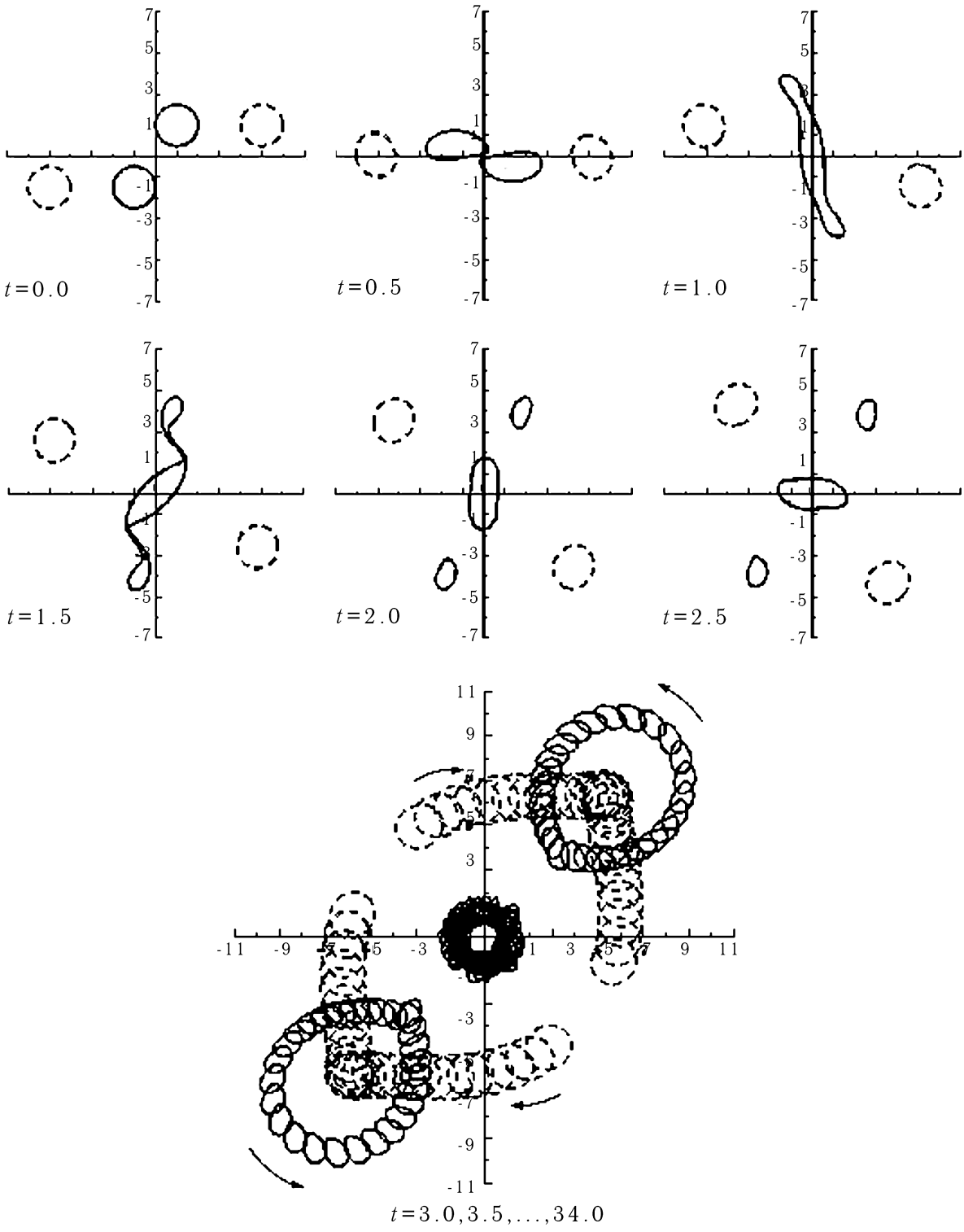

Fig. 17. Instantaneous configurations of vortex patches at $A = 3.0$, $B = 1.5$, $D = 2.0$, $\gamma = 3.0$

condition (2.5) for the vortices are still satisfied, the character of relative vortex motion undergoes only some quantitative modifications, and qualitative differences will be observed in the absolute motion. The appropriate problem requires special study.

Some considerations on the dynamics of the *distributed* hetons are given in the Appendix.

Acknoledgments

This research has been supported by INTAS (grant 94-3614); MAS was supported also by RFBR (grant 98-05-65446). The authors wish to thank V. V. Kozlov, A. V. Borisov, V. M. Gryanik, V. N. Zyryanov, A. N. Vulfson and G. N. Panin for the useful discussions.

Appendix

It is obvious, that the model of a point vortex cannot reflect all behavior peculiarities of a vortex with the final length in the horizontal direction. To make an approximative description of the baroclinic vortex we can use a two-layer structure of *vortex patches* — areas with constant vorticity located in each layer. If the centers of the vortex patches, forming a heton, are displaced relativly to each other, i. e. the two-layer vortex has a *tilted axis*, it is able to self-propel as the discrete two-layer pair. Contrary to their point analogs the distributed vortices have at least two distinctive peculiarities, namely:

1) Closely located with each other vortex patches of the same layer and the same sign have a property to merge in one vortex patch;

2) Under certain conditions a finite size circular vortex can be unstable with respect to small perturbations of its shape, what becomes the reason of its decay into smaller vortices.

There are elaborated methods of vortex patch modeling based on the optimally distributed discrete vortices [2]. However, in our opinion, the most effective method to study the evolution of finite size vortices is the so-called *Contour Dynamics Method* (CDM) [19]. The fact, known from hydrodynamics, that if there is no exterior influence, the velocity of any particle of an incompressible liquid on a plane is completely defined by the boundary configuration of the areas with piecewise constant distribution of a vortex, makes the ground for CDM. The generalization of CDM to the case of two-layer liquid is made in [11].

Using the algorithm given in [11], we studied the patterns of finite size heton interaction during their off-center collision, and have constructed the diagrams similar to those, that are given in Figure 6. Not dwelling here explicitly on obtained results, we would like to note, that the theory of point vortices is quite acceptable for description of barycentre behavior of the distributed vortices at small values of the parameter γ (small size vortex or strong stratification), or at rather large distances between vortex patches, as this is shown in the appropriate diagrams. Figures 16 and 17 demonstrate two examples of the most interesting characteristic features of the interaction process of the finite size vortices. Under each of the fragments of these figures the moments of dimensionless time are specified. In this case the time unit corresponds to the period of a fluid particle rotation along initially circular boundary of the unit radius vortex. The contours of the upper layer vortices are represented as solid lines, and lower layer vortex contours are represented as dashed lines.

Figure 16 demonstrates the evolution of a system formed of two distributed hetons, for each of them the initial axis tilt was small. Under the specified exterior parameters the process of interaction runs according the following script. In the initial stage of motion vortex patches of the upper layer approach each other rather close, but no merging between them has occurred. On the contrary the vortices of the lower layer, have merged at the same time, but in this case they divide right away into

three parts — central core and two peripheral vortices. Further, the division of each of the upper layer vortices into two practically equal parts happens. As a result, after destruction of the separated vortex lines, the rotational structure consisting of the following elements is formed:

a) A two-layer tripolar vortex rotating counter-clockwise develops in the central part of the configuration [10, 7, 17]; in this case the vortex consists of a lower layer cyclonic core and peripheral anticyclones in the upper layer;

b) On different sides of tripoles two non-compensated two-layer vortices move, obeying the condition of the central symmetry; they take part simultaneously both in translation and in rotary motions around "stronger" vortex patches in the lower layer (the ratio of areas of lower and upper vortex patches for these two-layer vortices is equal to 1.32). The configuration, as a whole, also perform cyclonic rotation induced by the central core (see arrows).

Thus, we can ascertain that the off-center collision of two hetons (at least on the computation time interval) causes formation of a vortex system of "solar system" type: the central cyclonic core in the lower layer plays the role of *the Sun*; *two planets* the anticyclones of the upper layer, orbited it in a close orbit; in a distant orbit *two more planets*, the cyclones of the lower layer, rotate. In their turn, they have *satellites*, the anticyclones of the upper layer.

Figure 17 demonstrates one more example of interaction of distributed hetons. Here also the central part of the configuration is occupied by a tripolar vortex. Now its core is a part of an anticyclone formed after merging of the upper layer vortex patches; subsequently small vortices separate from it. So, in this case, the core and surrounding lower layer cyclones, rotate clockwise. It is extremely interesting to examine the behavior of small upper layer vortices, separated from the core. During the time of computation these vortices have time to make a complete rotation around some peripheral points. Apparently, they are just those stagnation points, whose existence was postulated in the *hypothesis* formulated in Section 4.2.2. Besides, it can be seen from the figure, that there are also the braking points for the cyclonic vortices of the lower layer. We spoke previously about the limitations of the point vortex theory applied to the description of the distributed vortex behavior. We think that the last example points out the basic connection between point and distributed vortex approaches.

References

[1] *H. Aref, M. A. Stremler.* Four-Vortex Motion With Zero Total Circulation and Impulse. Phys. Fluids, 1999, A11, № 12, P. 3704–3715.

[2] *S. M. Belotserkovsky, A. S. Ginevsky.* Turbulent Jets and Wakes Simulation Using the Method of Discrete Vortices. Moscow, 1995, P. 369. (In Russian)

[3] *A. V. Borisov, I. S. Mamaev.* Poisson Structures and Lie Algebras in Hamiltonian Mechanics. Izhevsk, 1999, P. 464. (In Russian)

[4] *B. Eckhardt.* Integrable Four Vortex Motion. Phys. Fluids, 1988, 31, № 10, P. 2796–2801.

[5] *V. M. Gryanik.* Dynamics of Singular Geostrophic Vortices in a Two-Level Model of Atmosphere (Ocean). Izvestia, Atmos. Oceanic. Phys., 1983, 19, № 3, P. 227–240. (In Russian), P. 171–179. (English translation)

[6] *V. M. Gryanik, M. V. Tevs.* Dynamics and Energetics of Heton Interacting in Linearly and Exponentially Stratified Media. Izvestia, Atmos. Oceanic. Phys., 1997, 33, № 4, P. 419–433, (In Russian), P. 385–398. (English translation)

[7] *K. R. Helfrich, U. Send.* Finite-Amplitude Evolution of Two-Layer Geostrophic Vortices. J. Fluid Mech., 1988, 197, P. 331–348.

[8] *N. G. Hogg, H. M. Stommel.* The Heton, an Elementary Interaction Between Discrete Baroclinic Geostrophic Vortices, and its Implications Concerning Eddy Heat-Flow. Proc. Roy. Soc. London, 1985, A 397, P. 1–20.

[9] *N. G. Hogg, H. M. Stommel.* Hetonic Explosions: the Breakup and Spread of Warm Pools as Explaned by Baroclinic Point Vortices. J. Atmos. Sci., 1985, 48, P. 1465–1476.

[10] *M. Ikeda.* Instability and Splitting of Mesoscale Rings Using a Two-Layer Quasi-Geostrophic Model on a f-Plane. J. Phys. Oceanogr., 1981, 11, P. 987–998.

[11] *V. V. Kozlov.* General Theory of the Vortices. Izhevsk, 1998, P. 240. (In Russian)

[12] *V. F. Kozlov, V. G. Makarov, M. A. Sokolovskiy.* Numerical Model of the Baroclinic Instability of Axially Symmetric Eddies in Two-Layer Ocean. Izvestia, Atmos. Oceanic Phys., 1986, 22, № 8, P. 868– 874, (In Russian), P. 674–678. (English translation)

[13] *H. Lamb.* Hydrodynamics. 6th Ed, 1932, Dover, New-York, P. 732, (1947, OGIZ, Moscow-Leningrad, P. 931. (Russian translation)

[14] *E. A. Novikov.* Dynamics and Statistics of a System of Vortices. Sov. Phys. JETP, 1975, 41, P. 1868–1882, (In Russian), P. 937–943, (English translation)

[15] *J. Pedlosky.* Geophysical Fluid Dynamics. 2nd Ed, 1987, Springer-Verlag, New-York, P. 710.

[16] *N. Rott.* Constrained Three- and Four-Vortex Problems. Phys. Fluids, 1990, A2, № 8, P. 1477–1480.

[17] *M. A. Sokolovskiy, J. Verron.* Finite-Core Hetons: Stability and Interactions. J. Fluid Mech., 2000, 423, P. 127–154.

[18] *J. L. Synge.* On the Motion of Three Vortices. Can. J. Math., 1949, 1, P. 257–270.

[19] *N. J. Zabusky, M. N. Hughes, K. V. Roberts.* Contour Dynamics for Euler Equations in Two Dimensions. J. Comput. Phys., 1979, 30, № 1, P. 96–106.

[20] *S. L. Ziglin.* Nonintegrability of the Problem on the Motion of Four Point Vortices. Acad. Nauk. SSSR. Doklady, 1980, 250, № 6, P. 1296–1300. (In Russian)